Journal of Materials Chemistry A

Accepted Manuscript

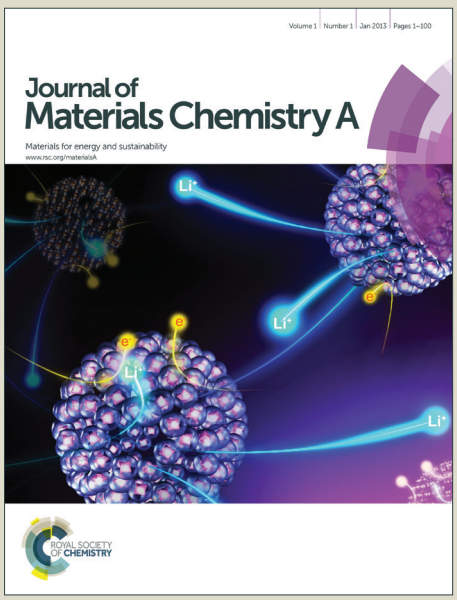

ROYAL SOCIETY OF CHEMISTRY

www.rsc.org/materialsA

Journal of Materials Chemistry A

Dynamic Article Links ►

Cite this: DOI: 10.1039/c0xx00000x

ARTICLE TYPE

www.rsc.org/xxxxxx

A High-Conduction Ge Substituted Li_3AsS_4 Solid Electrolyte with Exceptional Low Activation Energy

Gayatri Sahu[1], Ezhiylmurugan Rangasamy[1], Juchuan Li[2], Yan Chen[3], Ke An[3], Nancy Dudney[2], and Chengdu Liang[1*]

Received (in XXX, XXX) Xth XXXXXXXXX 20XX, Accepted Xth XXXXXXXXX 20XX
DOI: 10.1039/b000000x

Lithium-ion conducting solid electrolytes show potential to enable high-energy-density secondary batteries and offer distinctive safety features as an advantage over traditional liquid electrolytes. Achieving the combination of high ionic conductivity, low activation energy, and outstanding electrochemical stability in crystalline solid electrolytes is a challenge for the synthesis of novel solid electrolytes. Herein we report an exceptionally low activation energy (Ea) and high room temperature superionic conductivity via facile aliovalent substitution of Li_3AsS_4 by Ge, which increased the conductivity by two orders of magnitude as compared to the parent compound. The composition $Li_{3.334}Ge_{0.334}As_{0.666}S_4$ has a high ionic conductivity of 1.12 $mScm^{-1}$ at 27°C. Local Li^+ hopping in this material is accompanied by distinctive low activation energy Ea of 0.17 eV being the lowest of Li^+ solid conductors. Furthermore, this study demonstrates the efficacy of surface passivation of solid electrolyte to achieve compatibility with metallic lithium electrodes.

Introduction

In the current scenario of worldwide energy demands, efficient harvesting and delivery of renewable energy supplies are the future of sustainable energy production. Energy storage is critical to enable a stable supply of energy from available energy resources. With the current growth in need of portable consumer electronics, it demands much safer, high-density, light-weight, compact batteries. Although lithium-ion (Li-ion) batteries are widely used in portable electronics, their large scale application is still limited by low energy density, relative high cost of material production, and safety issues.[1, 2] Replacing carbonate based electrolytes by non-volatile and thermally stable solid electrolytes is one of the solutions to solve the crucial problems currently associated with liquid electrolytes[3-5] Although the solid electrolytes are non-flammable, their low ionic conductivities, relative high activation energy, and interfacial resistance hinder their practical applications.[6, 7]

In low ionic conducting solids the ions are usually trapped in their lattice sites and cannot escape although they vibrate continuously. Ionic conduction is easier at higher temperatures and especially if crystal defects and vacancies are present. It has been observed that substituting Ge on Li_3PS_4 results in a significant enhancement in conductivity, among the highest reported to date.[8] *Arsenic* being in the same group as *P* in the periodic table, and having larger radii than *P*, would show similar physical and chemical properties as *P*, the Li_3AsP_4 based compounds might increase the ionic conductivity with lower activation energy as compared to the Li_3PS_4 based compounds. The promising characteristics of this new composition could give rise to a highly conducting new solid electrolyte that will open up routes for synthesizing other possible compositions with similar or even better chemical and electrochemical properties. Selective aliovalent substitution in the crystal lattice creates solid solutions which introduces interstitial lithium ions or vacancies and leads to high ionic conductivities at room temperatures.[9]

The ionic conductivity of solid electrolytes usually changes dramatically with temperature because of their relatively high activation energy. Stable performance under changing temperature environments in a solid state device is a great challenge. Therefore, low activation energy in a material is crucial to achieve consistent performance of the device in a broad temperature range especially below room temperature.

The interfacial resistance is another important factor that cannot be ignored when it comes to their practical application in all-solid state devices. For example, a fast lithium superionic conductor $Li_{10}GeP_2S_{12}$ was reported by Kamaya *et al.* whose conductivity has reached 10^{-2} Scm^{-1} at room temperature.[8] Since, the lithium transference number in this solid electrolyte is unity; the lithium ion conductivity is even higher than carbonate based liquid electrolytes. However, their metallic Li compatibility still remains a challenge to be resolved.[8] Therefore, inspired by an already promising conductivity of $\sigma_{27^oC} = 1.31\times10^{-5}$ Scm^{-1} in Li_3AsS_4 compared to Li_4GeS_4, we synthesized the series of compositions in a general formula of $Li_{3+x}Ge_xAs_{1-x}S_4$ (where, x = 0 to 0.500) in order to investigate if desirable high ionic conductivity and low activation energy can be achieved in Ge

substituted Li_3AsS_4 compounds.

In this report, series of novel high conducting sulfide solid electrolytes have been reported which were achieved via aliovalent substitution of *Ge* on Li_3AsS_4. The highest conduction phase showed two-order increase in the ionic conductivity. This phase has the lowest reported activation energy in the lithium superionic conductors. Furthermore, the lithium compatibility was addressed with detailed study on the surface passivation by chemical treatment.

Experimental

Material Preparation

$[Li_{3+x}Ge_xAs_{1-x}S_4$ (where, x = 0 to 0.500)]

The starting materials of Li_2S (Sigma-Aldrich, 99.9% purity), GeS_2 (Sigma-Aldrich, 99.9% purity), and As_2S_5 (Sigma-Aldrich, 99.9% purity) were used as received. All materials were weighed, mixed in required molar ratios of Li_2S:As_2S_5:GeS_2 in an Ar-filled glove box, placed onto an Agate mortar and pestle and hand ground for 30 min. The molar ratios were determined keeping a trend in As to Ge ratio based on the two reactions given below:

$3Li_2S + As_2S_5 \rightarrow 2Li_3AsS_4$ (1)

$2Li_2S + GeS_2 \rightarrow Li_4GeS_4$ (2)

The powdery mixture was then carefully sealed in Pyrex glass tubes under house vacuum and heated at the reaction temperature of 550°C for 12 h in a furnace. The temperature was then decreased in a slow rate to 450°C in 12 h. After reacting, the tube was slowly cooled down to room temperature in 4 h.

Symmetric cell fabrication and Li cyclability measurements

Because of the chemical reaction of the solid electrolyte with metallic Li, the symmetric cell test was conducted on a passivated pellet. The passivation solution is a mixture of lithium borohydride and lithium iodide ($3LiBH_4$.LiI) with a molar ratio of 3:1 in tetrahydrofuran (THF).[10] The concentration is 5 wt. % of solid content in THF. The composition of the 3:1 molar ratio $LiBH_4$/LiI is expected to be a high-conduction solid electrolyte that is compatible with metallic Li.[10] The coating was applied by dipping the $Li_{3.334}Ge_{0.334}As_{0.666}S_4$ pellet into the composite solution and vacuum drying at 170°C for 1 h. Two pieces of Li foil were attached to the coated pellet for a symmetric cell test. The symmetric cells were cycled on a battery test system (Maccor 4000) with a current density of 0.1 $mAcm^{-2}$ at room temperature.

Structural characterization

Powder X-ray diffraction (XRD) patterns were collected on X'pert Pro Powder Diffractometer (PANalytical) with copper Kα line radiation (λ ≈ 1.5418 Å). The operating voltage and current were 45 kV and 40 mA respectively. The XRD characterization was handled with special care to avoid contact with air and moisture. Electron imaging was performed on a field emission scanning electron microscope (FESEM) (Zeiss Merlin) at 10 kV. The X-ray elemental maps were taken using the energy dispersive spectroscope (EDAX) detector attached to the FESEM system.

Property Measurements

Ionic conductivity measurements

All materials were cold pressed into dense pellets with sufficient mechanical strength for the measurements of ionic conductivity. Pellets (diameter 1.27 cm, thickness ~ 0.06 cm) were prepared by pressing the powder with carbon-coated aluminum foils (a sample from Exopack) on both sides in an argon-filled glove box. The carbon-coated aluminium foils served as blocking electrodes. Electrochemical impedance spectroscopy (EIS) measurements were carried out using a specially designed air-tight cell. The a.c. impedance measurements were conducted in the frequency range of 1 MHz to 1 Hz with the amplitude of 100 mV by using a frequency response analyser (Solartron 1260). An EIS spectrum is presented in Fig. S1. The Nyquist plot shows a typical semicircle at higher frequency region that represents the bulk and grain boundary resistance of the electrolyte and a spike at lower frequency region that represents the diffusion due to blocking electrode, a characteristic feature expected for pure ionic conductors. The intercept of the spike at the axis of Z'(Ω) was employed to determine the total ionic conductivity. For the Arrhenius plot, temperature was controlled between 25 to 100°C with 10°C intervals subsequent to 30°C in a temperature chamber (Maccor, ± 0.5 °C). To ensure the accuracy of measurements, every Arrhenius plot was measured by a forward scan from low to high temperature and a backward scan by reversing the temperature.

Electrochemical characterization

The cyclic voltammogram (CV) was measured on a $3LiBH_4$·LiI coated Li/ $Li_{3.334}Ge_{0.334}As_{0.666}S_4$/Pt cell where Li and Pt serve as the reference/counter and working electrode respectively. The potential was scanned from -0.5 to 5.0 V vs. Li/Li^+ at a scan rate of $1mVs^{-1}$ between -0.5V and 5.0 V at room temperature by using a potentiostat (Bio-Logic VMP3).

Electronic conductivity measurements

The DC polarization measurement was conducted to determine the electronic conductivity of the solid electrolyte. Each side of a cold pressed pellet (diameter 1.27 cm, thickness ~0.06 cm) was coated with 100 nm Au (99.9999%) serving as the blocking electrode. The pellet was sealed in a Swagelok cell in an Ar filled glove box. Conductivity measurements were carried out using a potentiostat (Bio-Logic VMP3) with a low-current probe where the lowest measurable current is smaller than 1 pA. The voltage was held at each step for 10 hours, and the stabilized current was recorded as an indication of the electronic conductivity. A Faraday cage was used during the measurement. The electronic conductivity and ionic transference number of $Li_{3.334}Ge_{0.334}As_{0.666}S_4$ were measured.

Results and discussion

Ge substitution on Li_3AsS_4 leads to super-ionic conductivity

Temperature dependence of the ionic conductivity of the samples for various molar ratios of As to Ge was studied. Fig. 1a represents typical Arrhenius plots for the Li-ion conductivity in the range of 25 to 100°C as a function of 1000/T for various molar ratios of the samples. The room temperature (RT) ionic conductivity achieved for the highest *Ge* concentration $Li_{3.500}Ge_{0.500}As_{0.500}S_4$ was 2.12×10^{-4} Scm^{-1} and for the lowest *Ge* concentration $Li_{3.286}Ge_{0.286}As_{0.714}S_4$ was 9.80×10^{-5} Scm^{-1}. The highest conductivity achieved across the entire temperature range was 1.12×10^{-3} Scm^{-1} at 25°C and 4.47×10^{-3} Scm^{-1} at 100°C for the composition $Li_{3.334}Ge_{0.334}As_{0.666}S_4$. When sulfides with compositions consisting of group IVA (Ge and Sn) and VA (P

and As) elements, the highest conduction phases are in a stoichiometric ratio of P:Ge, and P:Sn of 2:1,[8, 11] with one exception in the combination of As and Sn with stoichiometric ratio of As:Sn = 1:5.[12] A comparison with our results here reveals that the stoichiometric ratio of As:Ge = 2:1 is consistent with the previous reports [8, 11] and thus a higher Li^+ ion conductivity is expected.

To compare, the effect of Ge substitution on the conductivity of the material, pristine Li_3AsS_4 and Li_4GeS_4 were also synthesized using solid state synthesis route[6] and comparative analysis was carried out. The calculated AC impedance measurements and the Arrhenius plots were generated in the range of 25 to 100°C as a function of 1000/T. A clear observation in this plot is, the room temperature ionic conductivities of undoped Li_4GeS_4 and Li_3AsS_4 were 1.60×10^{-7} Scm^{-1} and 1.31×10^{-5} Scm^{-1} respectively. The conductivities of parent compounds were few orders of magnitude lower than the Ge substituted composition $Li_{3.334}Ge_{0.334}As_{0.666}S_4$. For solid electrolytes, introduction of foreign element into the crystal lattice via aliovalent substitution disrupts the regular ordered lattice of well-crystalline materials and therefore providing high concentration of defects and interstitials. Fine tuning of the lattice size and optimization of the carrier concentration in the skeleton framework by aliovalent cation substitution gave a superionic conductivity in mS/cm range.

An ideal solid electrolyte should be a pure ionic conductor, in which the lithium-ion transference number is 1. For sulfide based solid electrolytes the concern is the contribution of electronic conductivity to the total conduction of the solid electrolyte. In order to evaluate the transport properties of the Ge substituted Li_3AsS_4, The electronic conductivity was measured through the DC polarization measurements, which gave a value of 3.7×10^{-10} S cm^{-1}. The calculated Li^+ transference number is 0.9999, which is much higher than liquid and polymer electrolytes. In practical applications, the effective Li-ion conductivity determines the performance of the electrolyte. The effective conductivity of Li-ions is calculated by multiplying the total conductivity with the Li-ion transference number. A comparative analysis of various Li^+ transference numbers along with their effective Li^+ conductivities has been given in Table 1. Based on the data given, it is noteworthy that the solid electrolyte under study has an effective Li^+ conductivity comparable to the liquid electrolytes used in Li-ion batteries.

Impressive low activation energy E_a

A major factor influencing the ionic conductivity at different compositions is the activation energy for faster ion mobility because it corresponds to the energy barrier for ionic conduction. Changes in activation energy have been observed for a motion resulting from the increasing population of higher potential energy sites in the conduction network.[13] The activation energy is influenced by three factors, namely the vacancies, nature of bonds, and the site geometry. The activation energies E_a for the conduction were evaluated using the equation

$$\sigma_T = \sigma_o \exp(-E_a/k\beta T) \qquad (3)$$

Where, σ_T is the total electrical conductivity, σ_o is the pre-exponential parameter, T is absolute temperature, E_a is the activation energy and k_β is the Boltzmann constant. The E_a for conduction, calculated from the slope of an Arrhenius plot was 0.31 eV and 0.27 eV for $Li_{3.500}Ge_{0.500}As_{0.500}S_4$ and $Li_{3.286}Ge_{0.286}As_{0.714}S_4$ respectively. Whereas, Ea for the composition As:Ge = 2:1 i.e. $Li_{3.334}Ge_{0.334}As_{0.666}S_4$ was 0.17 eV, which is the lowest among all other molar ratio compositions. According to equation 3, the ionic conductivity is affected by temperature exponentially over the activation energy. A low activation energy ensures the least fluctuation of ionic conductivity with changing temperature conditions. Therefore the low activation energy favours the practical applications of solid electrolytes in a broad temperature range. In general, low activation energy for Li^+ hopping refers to more polarizable crystal lattice and easier ion migration. The nature of the substituted ion plays an important role in its mobility and activation energy. An optimum radius supports the ionic mobility in most structures. For example, the activation energy for larger

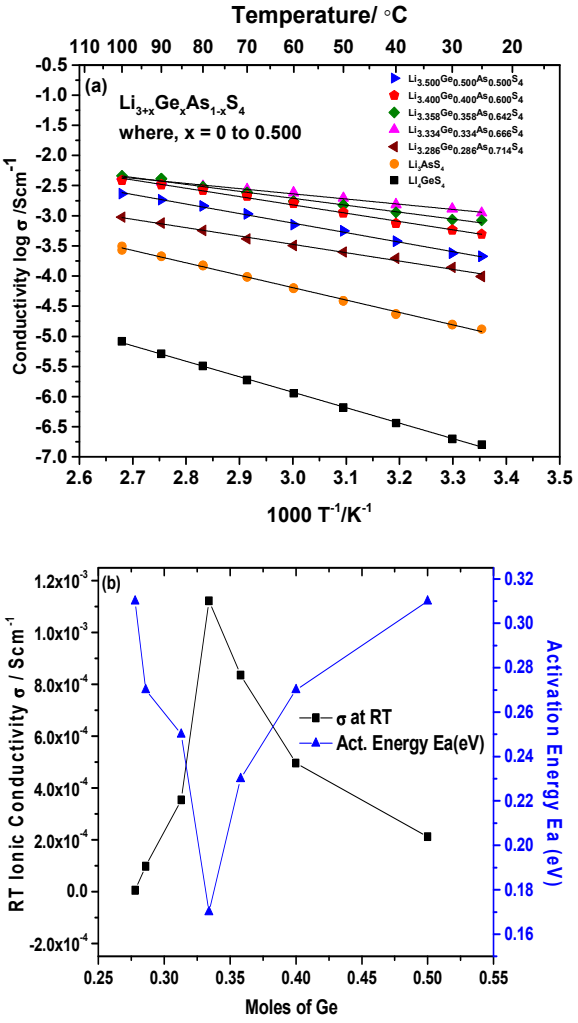

Fig.1 (a) Comparative arrhenius plot of ionic conductivity of Li_4GeS_4, Li_3AsS_4 and Ge substitued Li_3AsS_4, i.e. $Li_{3+x}Ge_xAs_{1-x}S_4$ (where, x = 0 to 0.500) with various molar ratios of As: Ge. **(b)** Ionic conductivity and activation energy vs. the molar ratios of As and Ge illustrating the improvement in ionic conductivity with decreasing concentration of Ge and the maximum conductivity was achieved with Ge = 0.334. An opposite trend can be observed for activation energy.

ions is lower than smaller ions.[14] The activation energy of $Li_{10}GeP_2S_{12}$ is 0.24 eV and going one element down the group with a slightly larger atomic radius with Arsenic in the same composition ratio $Li_{3.334}Ge_{0.334}As_{0.666}S_4$ it gives much lower E_a value of 0.17 eV. Unexpectedly the $Li_{3.334}Ge_{0.334}As_{0.666}S_4$ solid electrolyte has a lower ionic conductivity than $Li_{10}GeP_2S_{12}$, despite the lower barrier to ionic conduction. The low activation is most likely attributed to the high polarizability of the larger As atoms as compared to the small P atoms.

In order to understand more clearly the relation between various molar ratios of the substituent and host with that of their ionic conductivities and corresponding activation energies, a comparative analysis was carried out. Fig.1b represents plots of the composition vs. activation energy and the conductivity of the samples. There are mainly two features apparent in this plot. First, the calculated activation energy of the sample passes through a minimum value of 0.17 eV, at Ge molar conc. 0.334, and the composition dependence of activation energy corresponds to that of conductivity, indicating that changes in the conductivity are controlled by the changes in activation energy. Second, the clear trend in σ observed was that, it increases monotonously with increasing concentration of Ge from 0.27 to 0.33 in $Li_{3+x}Ge_xAs_{1-x}S_4$. It only holds good until the ratio reaches an equilibrium point at Ge = 0.334 after which any further increase in Ge concentration from 0.334 to 0.50 leads to inferior ionic conductivity. A comparison of activation energies of various solid electrolytes both sulfides[8, 12, 15, 16] and oxides[17-19] has been given in Fig.2. The E_a for the composition $Li_{3.334}Ge_{0.334}As_{0.666}S_4$ showed the lowest value among all the Li ion conductors which is comparable to the activation energy of an extensively studied high conduction sodium ion conductor sodium β-alumina[20] and a recently reported glass ceramic conductor.[21]

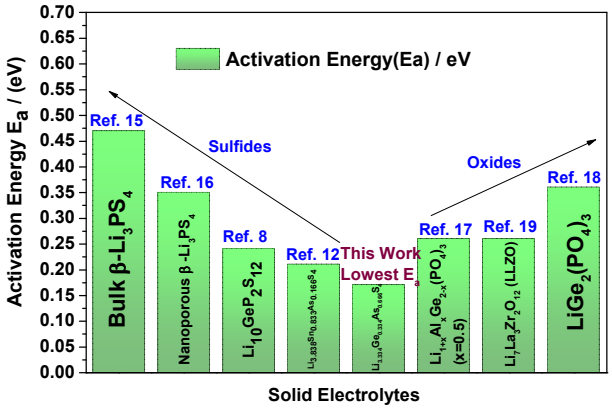

Fig.2 Solid electrolytes (sulfides and oxides) and their individual activation energies

Effect of Ge substitution on Li_3AsS_4 towards solid solution formation

In aliovalent substitution, solid solutions are formed when ions are substituted by other ions of different valence or charge, which consequently causes additional changes in the lattice such as (i) creation of interstitials or vacancies, or (ii) introduction of electrons or holes to preserve the electron neutrality. It is more reasonable to assume the former condition applies in this case since no transition elements exist as a constituent of the solid electrolyte $Li_{3+x}Ge_xAs_{1-x}S_4$ (where, x = 0 to 0.500) which would contribute to the creation of electrons or holes in the composition. In order to further explain the cause of the variation in conductivity behaviour according to the concentration of substituent under identical synthesis conditions, specific

Table 1. Comparison of Li^+ transference number and effective Li^+ conductivity of various electrolytes

Electrolytes	Type of Electrolyte	Li transference number Li t^+	Corresponding σ (S/cm)	Effective Li^+ conductivity	References
N-butyl-N-methyl-pyrrolidinium bis(trifluoromethanesulfonyl)imide (BMP-TFSI) + lithium bis(trifluoromethanesulfonyl)imide (Li-TFSI)	Liquid	0.132	1.17×10^{-2}	1.54×10^{-3}	13
LiPF6 in PC/EC/DMC	Liquid	0.38	1.00×10^{-2}	3.80×10^{-3}	14
$LiClO_4$ dissolved in PEO	Polymer	0.56	5.40×10^{-6}	3.02×10^{-6}	15
PEO network electrolyte	polymer	0.98	6.90×10^{-7}	6.76×10^{-7}	15
Li3.838Sno.833Aso.166S4	Solid electrolyte	0.9999	1.39×10^{-3}	1.39×10^{-3}	12
Li3.334Geo.334Aso.666S4	Solid electrolyte	0.9999	1.12×10^{-3}	1.12×10^{-3}	This work

structural characterization of the crystal structure was taken. **Fig. 3** shows a comparative analysis of XRD spectra of various compositions of the solid electrolytes with systematic variation in the dopant concentration. The XRD patterns of the $Li_{3+x}Ge_xAs_{1-x}S_4$ (where, x = 0 to 0.500) synthesized in the present study show that the as synthesized powders are well-crystallized with a strong x-ray diffraction peak at 2θ = 17.04° and other prominent diffraction peaks at 2θ = 25.76° for all the compositions. All XRD patterns (Fig. 3) show that the matrix of $Li_{3+x}Ge_xAs_{1-x}S_4$ (where x = 0 to 0.5) is Li_3AsS_4, orthorhombic crystal structure. A series of peaks from 2θ of 10 to 35 are assigned for Li_3AsS_4 as follows: 12.8 (010); 13.05 (100); 17.23 (210); 17.98 (101); 19.29 (110); 22.38 (111); 22.87 (002); 26.15 (012); 26.48 (020); 28.41 (200); 29.84 (112); 30.15 (120); 32.26 (121); 33.50. (211); and 34.41 (003). The other prominent peaks are at 39.07 (212); 44.51 (222); 46.69 (032), and 51.42 (312).

The peaks for the crystal structure Li_4GeS_4 can be compared with the literature data reported elsewhere.[22] Apart from these peaks, there are additional peaks appearing at 2 theta 14.40°, 15.59°, 42.05° and 49.53° which indicate solid solutions arising from the *Ge* substitution on Li_3AsS_4. The patterns also show unknown peaks at 27.46° and 45.85° which can be attributed to new phases in the lattice. The substitution creates interstitials or vacancies that are accounted for the enhanced ionic conductivity in Ge substituted samples. In heterovalent or aliovalent substitution, if the replaceable cation of the tetrahedral center of the anion *i.e.*$[AsS_4]^{3-}$ has lower charge than that of the dopant *i.e.* $[GeS_4]^{4-}$ then, vacancies are created in order to preserve the electroneutrality.[23] The vacancies enhance the overall conductivity of the material.

Artificial solid electrolyte interphase (ASEI) protects the super-ionic conductor

The impressive feature of an all-solid-state battery with solid electrolyte is that it can employ a Li metal without the deleterious dendritic Li deposition typically seen in Li cells employing organic liquid electrolytes. Although some recently discovered sulfide-based solid electrolytes have sufficient ionic conductivity comparable to that of liquid electrolytes, the metalloids Ge and Sn that impart the high Li-ion conductivity cause the incompatibility of these new materials with metallic Li. This work does not show an exception to the incompatibility with metallic Li. Taking the advantage of its solid form, it is possible to modify or passivate the surface of the electrolyte to achieve good compatibility with metallic Li. We have previously shown the concept of passivating the solid electrolyte by using a facile surface coating technique.[12] The approach here was the same to chemically passivate the surface of the solid electrolyte pellet of $Li_{3.334}Ge_{0.334}As_{0.666}S_4$ with a Li-compatible composite of $3LiBH_4{\cdot}LiI$ in THF solvent.[10] The THF was removed by heating the coated pellet up to 170°C. We further investigated this surface passivation phenomenon by morphological analysis via FESEM imaging and EDAX x-ray mapping techniques. Fig. 4 shows FESEM images and elemental maps of the $3LiBH_4{\cdot}LiI$ surface coated $Li_{3.334}Ge_{0.334}As_{0.666}S_4$ pellet. A passivation layer was observed on the solid electrolyte surface. The pellet has a total thickness estimation of ~750 µm with a coating thickness of ~ 20 µm each side. The representative FESEM images in Fig. 4 (a & b) confirm that the coating forms a homogeneous and continuous protective layer throughout the pellet surface. A close examination of the roughened surface revealed a visible texture difference between the $Li_{3.334}Ge_{0.334}As_{0.666}S_4$ and the $3LiBH_4.LiI$ layer. The protective layer acts as a dense artificial solid electrolyte interphase (ASEI) between the solid electrolyte and the reactive lithium metal. The X-ray mapping results presented in Fig. 4 (c-f) reveals the ASEI is spatially distributed. Iodine is most prominently present at the edges whereas it is almost absent at the body of the pellet. Likewise, the principal elements Germanium, Arsenic, and Sulfur are discretely distributed throughout the pellet surface except the edges where, Iodine is in highest concentration. There is no doubt that such a dense passivation layer can effectively block the access of the solid electrolyte with metallic lithium and eliminate cell shunting path(s). The EDAX x-ray maps and the FESEM micrographs reveal that the ASEI on the pellet is a very useful tool in addressing the surface engineering of the solid electrolyte pellet to impart lithium metal compatibility.

Shown in Fig. 5a is a comparison of the symmetric cell cycling data with and without coating. The pristine pellet is not compatible with metallic Li electrodes. The cell voltage is spiky as a result of the interfacial reaction between the solid electrolyte and the newly deposited metallic Li. The polarization voltage profile shows continuous increase in potential in the later cycles which could be due to further increased interfacial resistance between lithium and the solid electrolyte. A smooth cell voltage with very minimal interfacial resistance was achieved after the $3LiBH_4{\cdot}LiI$ coating was applied. The coating material $3LiBH_4{\cdot}LiI$, is a good ionic conductor that is compatible with metallic Li.

The compatibility of the coated electrolyte with metallic lithium was further proved by the cyclic voltammetry (CV) measurement of Li/$Li_{3.334}Ge_{0.334}As_{0.666}S_4$/Pt cell. The data has been shown in

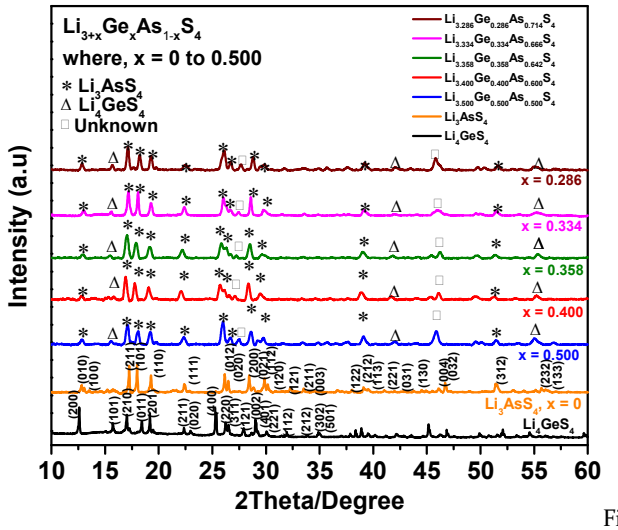

Fig.3 Structural evaluation. XRD patterns of Li_4GeS_4 and Ge substituted Li_3AsS_4, i.e. $Li_{3+x}Ge_xAs_{1-x}S_4$ (where, x = o to o.5oo) showing solid solution formation with Ge substitution on Li_3AsS_4

Fig. 5b. Li was the working and pseudo reference electrode and Pt was the counter electrode. The potential was scanned from -0.5 to 5.0 V vs. Li/Li^+ at a scan rate of $1mVs^{-1}$. The superionic $Li_{3.334}Ge_{0.334}As_{0.666}S_4$ SE has a broad electrochemical window up to 5V. The cathodic current occurred right at 0V. This fact indicates that no side reaction occurred during the lithium deposition. A sharp anodic peak was observed between 0 and 0.3V referring to lithium striping. No additional peak was observed in the entire 5V electrochemical window. As opposed to the CV data of an uncoated pellet cycled under similar conditions did not show any oxidation or reduction reactions after cycling (Fig.5b). Furthermore, to observe the chemical compatibility after surface coating, post-mortem analysis was carried out on pellets with and without $3LiBH_4 \cdot LiI$ coating. One digital image of the pellet after cycling is shown in Fig. S2 with strong reaction of lithium metal on an uncoated pellet as opposed to no reaction of lithium on a surface passivated pellet.

This experiment opens up new directions for solving the

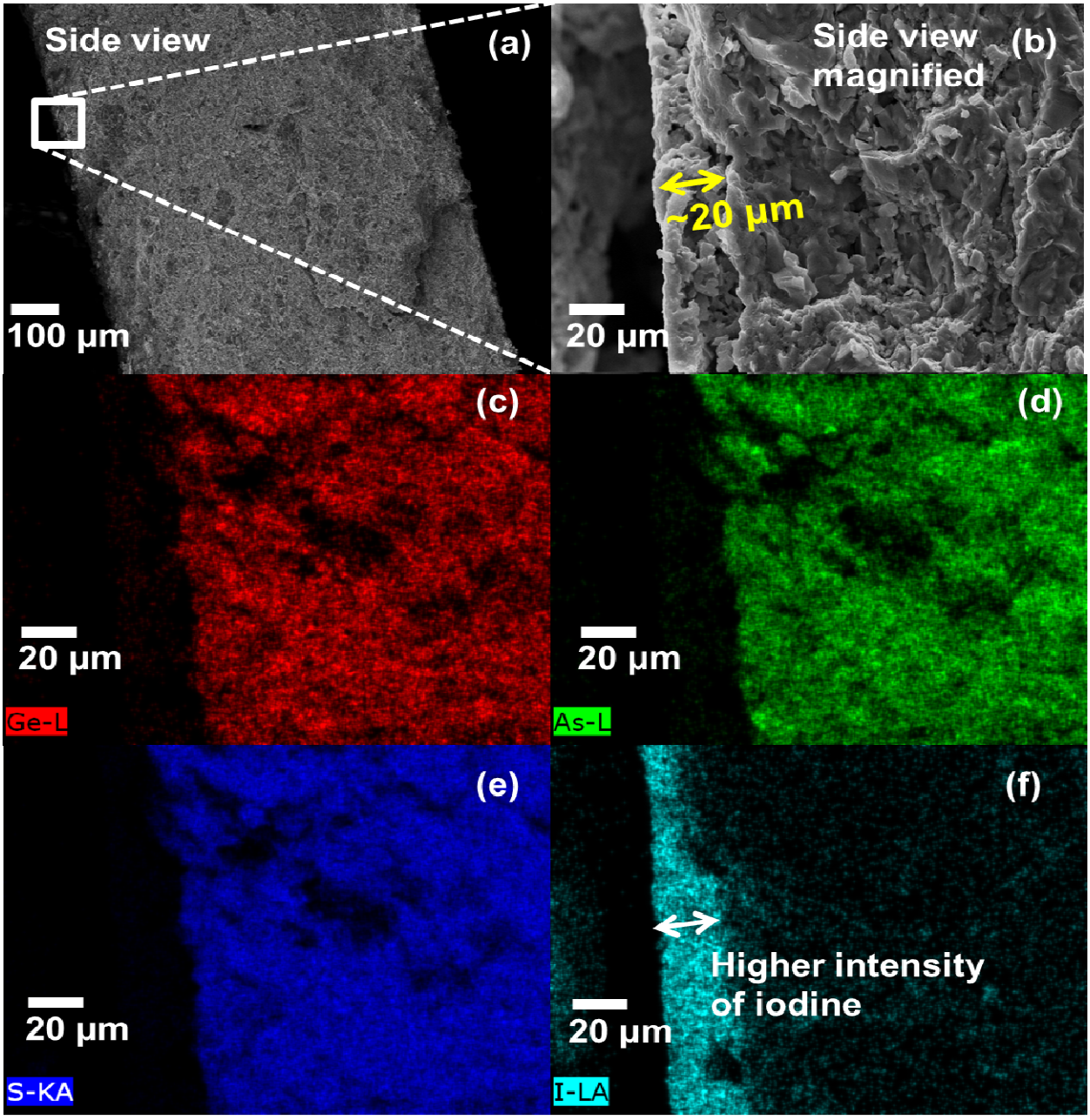

Fig.4 Scanning electron microscopy images (a & b) and EDAX elemental maps of Ge, As, S, and I of the $3LiBH_4$+LiI coated $Li_{3.334}Ge_{0.334}As_{0.666}S_4$ pellet (c-f) respectively. Maps collected at 20 eV.

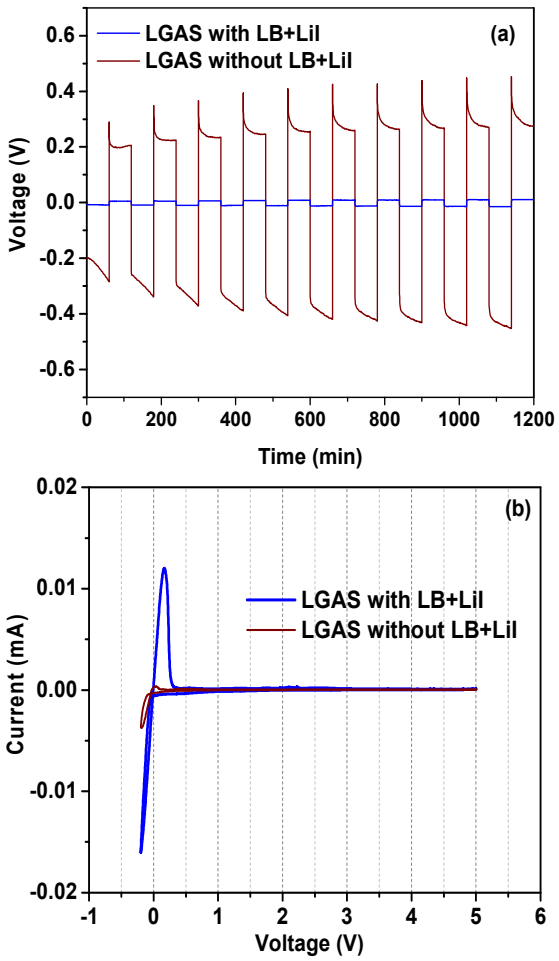

Fig.5 (a) Li/ $Li_{3.334}Ge_{0.334}As_{0.666}S_4$/Li symmetric cell with and without $3LiBH_4$·LiI (LB+LiI) coating showing lithium cyclability at a current density of 1mA/cm^2 at ambient conditions (25^{o}C), (b) CV with and without $3LiBH_4$·LiI coated on Li/$Li_{3.334}Ge_{0.334}As_{0.666}S_4$/Pt cell, where Li and Pt serve as the reference/counter and working electrode respectively.

compatibility issues of high-conduction Li-ion conductors. The results suggest there are possible materials like $3LiBH_4$·LiI which can be compatible with lithium and still remain intact and highly protective during the cycling of the battery.

Conclusions

Crystalline electrolytes of $Li_{3+x}Ge_xAs_{1-x}S_4$ were prepared by mechanical mixing and subsequent heat treatment in the composition range $0 \le x \le 0.5$. All the resulting crystals showed higher conductivity than their parent counterparts, the room temperature conductivity increased with increasing the Ge concentration and it was reached to 1.12×10^{-3} Scm^{-1} at a substitution level of 33.4 % of Ge on the Li_3AsS_4 lattice. The resulted phase $Li_{3.334}Ge_{0.334}As_{0.666}S_4$ showed Li^+ transference number 0.9999 showing Li^+ as the only mobile species. The activation energy E_a of this phase was 0.17 eV which was one of the lowest activation energy E_a among the lithium-ion conductors. Such exceptional low activation energy suggests this electrolyte would show steady performance in a device under broad temperature range. Although chemical compatibility with metallic Li was compromised by the Ge and As atoms, surface passivation of the solid electrolyte resulted in protective ASEI layer which preserves the solid electrolyte surface and eliminates the possibilities of interfacial reactions and therefore impart excellent cyclability with metallic Li. The surface passivated phase $Li_{3.334}Ge_{0.334}As_{0.666}S_4$ showed excellent lithium cyclability and had wide electrochemical window up to 5V vs. Li^+/Li. These results demonstrate that the optimum synthesis conditions and surface engineering with suitable material choices can produce high conduction sulphide-based solid electrolytes with desirable properties. The application of this high conduction solid electrolyte in high-performance all-solid-state batteries is currently in progress.

Acknowledgment

This work was sponsored by the Division of Materials Sciences and Engineering, Office of Basic Energy Sciences US Department of Energy (DOE). The synthesis and characterization of materials were conducted at the Center for Nanophase Materials Sciences, which is sponsored at Oak Ridge National Laboratory by the Scientific User Facilities Division, US DOE.

Notes and references

(1) Center for Nanophase Materials Sciences; e-mail: liangcn@ornl.gov
(2) Materials Science and Technology Division, Oak Ridge National Laboratory, Oak Ridge, TN 37831-6493, USA
(3)Spallation Neutron Sources, Oak Ridge National Laboratory, Oak Ridge, Tennessee 37831, USA.

† Electronic Supplementary Information (ESI) available: [details of any supplementary information available should be included here]. See DOI: 10.1039/b000000x/

References

1. Q. S. Wang, P. Ping, X. J. Zhao, G. Q. Chu, J. H. Sun and C. H. Chen, *Journal of Power Sources*, 2012, 208, 210-224.
2. M. Venables, *Engineering & Technology*, 2013, 8, 24-25.
3. J. W. Fergus, *Journal of Power Sources*, 2010, 195, 4554-4569.
4. P. Knauth, *Solid State Ionics*, 2009, 180, 911-916.
5. K. Takada, *Acta Materialia*, 2013, 61, 759-770.
6. R. Kanno, T. Hata, Y. Kawamoto and M. Irie, *Solid State Ionics*, 2000, 130, 97-104.
7. T. Kaib, P. Bron, S. Haddadpour, L. Mayrhofer, L. Pastewka, T. Järvi, M. Moseler, B. Roling and S. Dehnen, *Chem. Mater., Article ASAP*, 2013, DOI: 10.1021/cm400541n.
8. N. Kamaya, K. Homma, Y. Yamakawa, M. Hirayama, R. Kanno, M. Yonemura, T. Kamiyama, Y. Kato, S. Hama, K. Kawamoto and A. Mitsui, *Nat. Mater.*, 2011, 10, 682-686.
9. A. R. West, in *Solid State Electrochemistry*, ed. P. G. Bruce, Cambridge University Press, Cambridge, U.K. , 1995.
10. H. Maekawa, M. Matsuo, H. Takamura, M. Ando, Y. Noda, T. Karahashi and S. I. Orimo, *Journal of the American Chemical Society*, 2009, 131, 894-895.
11. P. Bron, S. Johansson, K. Zick, J. S. a. d. Günne, S. D. and and B. Roling, *J. Am. Chem. Soc*, 2013, 135, 15694–15697.

12. G. Sahu, Z. Lin, J. Li, Z. Liu, N. Dudney and C. Liang, *Energy & Environmental Science*, 2014, 7, 1053-1058.
13. A. C. M. Rodrigues and M. J. Duclot, *Solid State Ionics*, 1988, 28, 729-731.
14. B. G. Silbernagel and M. S. Whittingham, *Journal Chemical Physics*, 1976, 64, 3670.
15. M. Tachez, J. P. Malugani, R. Mercier and G. Robert, *Solid State Ionics*, 1984, 14, 181-185.
16. Z. Liu, W. Fu, E. A. Payzant, X. Yu, Z. Wu, N. J. Dudney, J. Kiggans, K. Hong, A. J. Rondinone and C. Liang, *J Am Chem Soc.*, 2013, 135, 975–978.
17. J. S. Thokchom and B. Kumar, *Journal of Power Sources*, 2008, 185, 480-485.
18. J. Fu, *Solid State Ionics*, 1997, 104, 191-194.
19. E. Rangasamy, J. Wolfenstine and J. Sakamoto, *Solid State Ionics*, 2012, 206, 28-32.
20. A. R. West, *Basic Solid State Chemistry* Wiley & Sons, Incorporated, John, Second edn., 1999, Paperback, Revised.
21. Yoshikatsu Seino, T. Ota, K. Takada, A. Hayashi and M. Tatsumisago, *Energy and Environmental Science*, 2014, 627–631.
22. M. Murayama, R. Kanno, Y. Kawamoto and T. Kamiyama, *Solid State Ionics*, 2002, 154, 789-794.
23. A. R. West, *Basic Solid State Chemistry*, Wiley; 2nd edition, August 3, 1999.

Graphical Abstract

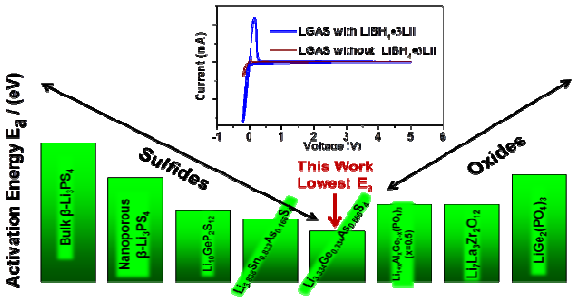

A Li-ion conductor with an ultralow activation energy.